Determination of the Guest Radius of Gyration in Polymer Blends: Time-Resolved Measurements of Excitation Transport Induced Fluorescence Depolarization

M. D. Ediger,† R. P. Domingue, K. A. Peterson, and M. D. Fayer*

Chemistry Department, Stanford University, Stanford, California 94305.
Received August 27, 1984

ABSTRACT: An experimental study of polymer blend structure using electronic excitation transport induced fluorescence depolarization is presented. Copolymers of vinylnaphthalene and methyl methacrylate in poly(methyl methacrylate) (PMMA) and poly(ethyl methacrylate) (PEMA) hosts are examined. It is shown that recent theoretical treatments accurately describe the time dependence of the fluorescence depolarization caused by excitation transport among chromophores on isolated polymer coils. Analysis of the experimental results strongly suggests that if an appropriate pair correlation function is employed, quantitative determination of coil size (the root-mean-square radius of gyration, $\langle R_g^2 \rangle^{1/2}$) will be possible. Comparisons are made between the size of the copolymer in PMMA and PEMA hosts and in different molecular weight PMMA hosts. The technique is capable of examining blends in which the guest concentration is very small, a regime which is difficult to investigate with previous methods. When the concentration of copolymer in PEMA is increased, phase separation occurs and is manifested by an increased rate of fluorescence depolarization (increased rate of excitation transport) and a decreased fluorescence lifetime due to trapping.

I. Introduction

The nature of intermolecular interactions determines the microscopic structure of condensed phase systems. For a relatively small molecule with basically fixed molecular framework, the structure of an ensemble of molecules is, nonetheless, very complex, e.g., the structure of liquid water or the crystal structure of naphthalene. However, if the molecules of interest are macromolecules, the structural problem has an additional dimension of complexity. A polymer coil in a solution or in a solid polymer blend has a vast number of possible configurations. The interaction of a polymer coil with its environment determines its macroscopic structure, while the local structure (chain segment geometry) determines the nature of the coil–environment interactions. Thus, the problem of polymer structure involves an interplay between thermodynamic interactions and possible coil configurations. Understanding this interplay is of fundamental importance in understanding polymeric materials.

Polymer blends are also of tremendous technological importance. This is due in large part to the fact that the bulk properties of a blend can be carefully controlled by adjusting the composition of the various components. These properties are critically dependent on the mixing of blend components on a molecular level. Phase separation into domains of various compositions can occur as a result of unfavorable intermolecular interactions between the different polymers present. A very sensitive indicator

†Permanent address: Department of Chemistry, University of Wisconsin, Madison, WI 53706.

0024-9297/85/2218-1182$01.50/0

of the interactions between two polymers is the root-mean-square radius of gyration ($\langle R_g^2 \rangle^{1/2}$) of one polymer dispersed in a matrix of the other.

In this paper we describe time-resolved fluorescence depolarization measurements of excitation transport among chromophores on isolated polymer coils. As has been noted in several recent theoretical papers,[1-6] these measurements allow the determination of $\langle R_g^2 \rangle^{1/2}$ and other quantities related to coil structure.

In addition to its utility in probing polymer and polymer blend structure, excitation transport among chromophores attached to a polymer backbone may be important in its own right. Clustering chromophores in a small volume, e.g., on an isolated coil or in small phase-separated domains in a polymer blend, leads to highly efficient energy transport in a manner akin to the clustered chromophores in a naturally occurring photosynthetic unit. Thus, specially tailored polymer blends may be useful in solar energy conversion.

Qualitatively it is easy to appreciate the relationship between polymer coil size, $\langle R_g^2 \rangle^{1/2}$, and the rate of excitation transport. If isolated polymer coils containing a small fraction of chromophores are dispersed in a host polymer with which they have favorable thermodynamic interactions, they will assume extended configurations with a large average interchromophore separation. Since the rate of excitation transport is a strong function of distance, an extended configuration results in a relatively slow rate of transport. If the guest polymer–host polymer interactions are less favorable, the isolated coils will contract and excitation transport will become more probable. As excitation transport becomes faster, the polarization of the fluorescence emitted by the chromophores will decay more quickly. The detailed relationship between the experimental observables and $\langle R_g^2 \rangle^{1/2}$ is discussed in section II.

In section IV we report the results of excitation transport measurements on copolymers of methyl methacrylate and 2-vinylnaphthalene dispersed in poly(methyl methacrylate) (PMMA) and poly(ethyl methacrylate) (PEMA) hosts. Excitation transport among the naphthalene groups allows the miscibility of the blend to be investigated and $\langle R_g^2 \rangle^{1/2}$ for the copolymer to be determined. The copolymer/PMMA blends were miscible at all concentrations investigated. Comparison to recent theoretical work[1,5] allows the determination of $\langle R_g^2 \rangle^{1/2}$ for the copolymer in PMMA hosts of two different molecular weights. Both theoretical treatments correctly describe the time dependence of the excitation transport. When the pair correlation function for the copolymer chain is appropriately related to the theoretical treatments, the experimental value for $\langle R_g^2 \rangle^{1/2}$ is in agreement with determinations by other methods.

We also performed fluorescence depolarization measurements of excitation transport in blends of the copolymer and PEMA. These experiments indicate miscibility only at copolymer concentrations below about 0.1%. This is confirmed by the concentration dependence of emission features which are probably due to interchain alkylnaphthalene dimers.

The motivation for a new method of looking at the structure of polymer blends comes from the limitations of current techniques. The most common experimental method used to determine the $\langle R_g^2 \rangle^{1/2}$ of isolated polymer coils in the solid state is neutron scattering. Although this technique has yielded considerable insights into the nature of polymeric solids,[7] it has several disadvantages. Sample preparation is difficult, a neutron source is required, and the technique cannot be used with very low concentrations (<1%) of the polymer of interest. This last limitation is of particular importance since many polymer blends are phase separated even at this relatively low concentration. In these cases neutron scattering cannot provide information about the behavior of isolated chains.

The limitations of neutron scattering have created an interest in the use of fluorescence techniques which examine properties of polymeric solids. Fluorescence, since it can be detected against a dark background, can be used to investigate the properties of a minor component in a blend at concentrations at least several orders of magnitude lower than that which can be detected in a neutron-scattering experiment. This is important for blends which have a strong tendency to phase separate. Very little work has been done on such systems with neutron scattering. As a result, very little is known about how $\langle R_g^2 \rangle^{1/2}$ is changed from its value under Θ-conditions.

Several techniques which use fluorescence to monitor excitation transport have been applied to the study of polymer blends. Excimer fluorescence (resulting from excitation transport) has been used to investigate blend miscibility, phase diagrams, and the kinetics of spinodal decomposition.[8,9] Excitation transport and trapping have been used to study the effects of freeze-drying on blend structure.[10] These techniques are sensitive to the local concentration of chromophores and as a result are sensitive to aggregation and phase separation. The fluorescence depolarization technique used in the experiments reported here shares this characteristic. This technique is unique, however, in that it provides a quantitative measure of $\langle R_g^2 \rangle^{1/2}$.

II. Theory and Experimental Observables

The rate of excitation transport between the two chromophores is given by

$$\omega = (R_0/r)^6/\tau \tag{1}$$

where τ is the excited-state lifetime, r is the distance between the chromophores, and R_0 is the critical transfer radius for excitation transport.[11] Equation 1 is the orientation-averaged dipole–dipole interaction. The inclusion of orientation effects is discussed in Appendix A.

The fundamental quantity of theoretical and experimental interest is $G^s(t)$, the ensemble average probability that an excitation is on the originally excited chromophore at time t.[12] In this section we describe how the experimental $G^s(t)$ can be obtained from fluorescence depolarization data. We will also briefly describe the two theoretical calculations of $G^s(t)$ which will be compared to the data.

If a sample of randomly oriented chromophores is excited by a short pulse of polarized light, the decay of the polarized fluorescence components can be written as

$$I_{\parallel}(t) = e^{-t/\tau}(1 + 2r(t)) \tag{2}$$

$$I_{\perp}(t) = e^{-t/\tau}(1 - r(t)) \tag{3}$$

$I_{\parallel}(t)$ and $I_{\perp}(t)$ are the time-dependent fluorescence intensities polarized parallel and perpendicular to the polarization of the exciting light, respectively. In these equations τ is the excited-state lifetime and $r(t)$ is the fluorescence anisotropy.

$r(t)$ contains information about all time-dependent sources of depolarization. In the experiments reported in this paper depolarization occurs due to excitation transport and, to a very slight extent, due to motion of the chromophores. For this case

$$r(t) = CG^s(t)\Phi(t) \tag{4}$$

where $\Phi(t)$ is the rotational correlation function and C is

a time-independent constant which describes the degree of polarization of the transitions involved. Because the samples used in these experiments were far below the glass transition temperature (T_g), $\Phi(t)$ is close to unity for all times examined.

In order to obtain $G^s(t)$, depolarization measurements must be performed on two copolymers. These copolymers differ only in the fraction of chromophores on the chain. Copolymer 1 has such a small fraction of chromophores that excitation transport is negligible ($G^s(t) = 1$). Copolymer 2 has an appreciable fraction of chromophores, so both excitation transport and a small amount of chromophore motion contribute to $r(t)$. $r(t)$ for either copolymer is obtained as follows:

$$r(t) = \frac{I_\parallel(t) - I_\perp(t)}{I_\parallel(t) + 2I_\perp(t)} \tag{5}$$

Let $r_1(t)$ and $r_2(t)$ represent the anisotropies for copolymer 1 and copolymer 2, respectively. The $G^s(t)$ for copolymer 2 (with an appreciable fraction of chromophores) will be given by

$$G^s(t) = r_2(t)/r_1(t) \tag{6}$$

We obtain a value of $\langle R_g^2\rangle^{1/2}$ for copolymer 2 by comparing the above experimental $G^s(t)$ with a theoretical calculation of $G^s(t)$. There are two calculations of $G^s(t)$ in the literature. Ediger and Fayer[1] (EF) have performed a model calculation for an ensemble of isolated chains with a given $\langle R_g^2\rangle^{1/2}$. EF take the subset of all configurations with a given R_g to be described as chromophores randomly distributed within a sphere of radius R (R is chosen such that the second moment of the chromophore distribution is R_g). $G^s(t)$ is calculated for this R_g and then averaged over the Flory–Fisk distribution function for R_g. This average yields $G^s(N,\langle R_g^2\rangle^{1/2},t)$, where the explicit dependence on $\langle R_g^2\rangle^{1/2}$ and N, the number of chromophores on the chain, has been indicated.

Fredrickson, Andersen, and Frank[2-6] (FAF) have used a different model to calculate $G^s(t)$. FAF use a nonperturbative calculation to obtain $G^s(t)$ for an ideal, infinite chain. Their treatment allows for transport between coils as well as within a coil, and for the presence of excitation traps composed of chemically distinct species on the chain. (For comparison with the data in this paper we will set the trap concentration to zero and use only their results in the limit of low guest concentrations where interchain transport does not occur.)

Appendix A contains the equations used to calculate $G^s(t)$ for both the EF and FAF theories. Both theories have only one adjustable parameter which can be directly related to $\langle R_g^2\rangle^{1/2}$.

III. Experimental Techniques

Polymer Materials. Two copolymers of methyl methacrylate and 2-vinylnaphthalene were used in the fluorescence depolarization measurements. A copolymer with a very small fraction of 2-vinylnaphthalene monomers (mole fraction = 0.0015, molecular weight $\simeq$ 50 000) was used to assess the depolarization due to chromophore motion. This copolymer was synthesized in analogy to the procedure of Fox et al.[14] A second copolymer (mole fraction 2-vinylnaphthalene = 0.10, molecular weight $\simeq$ 20 000) was used to determine depolarization due to both excitation transport and molecular motion. This copolymer was the generous gift of Professor C. W. Frank, Stanford Chemical Engineering Department.

The host materials for these experiments consisted of commercially available samples of poly(methyl methacrylate) (PMMA) and poly(ethyl methacrylate) (PEMA): (1) PMMA, Scientific Polymer Products No. 424, Lot No. 02, molecular weight = 12 000 (manufacturer's value, light scattering); (2) PMMA, Polysciences No. 4553, molecular weight $\simeq$ 120 000; (3) PEMA, Du Pont Elvacite Grade 2042, molecular weight $\simeq$ 120 000; (4) PEMA, Du Pont Elvacite Grade 2043, Lot No. 275035, molecular weight $\simeq$ 12 000. Unless otherwise noted the molecular weight was determined by viscosity measurements. Since the polydispersity of the materials was not known, the molecular weight values are only approximate.

Sample Preparation. Samples were prepared by solvent casting or by molding under pressure above T_g. For the molded samples the appropriate guest and host polymers were dissolved in benzene in the desired proportion (total polymer concentration was about 5%). This solution was then frozen at 77 K and allowed to warm to room temperature under a vacuum yielding a fluffly white solid. This material was placed in a stainless steel piston which was evacuated and quickly heated to about 20 °C above T_g. (We found that quickly heating the freeze-dried material decreased unwanted fluorescence from the host polymer.) After 20 min at this temperature the sample was subjected to 10 000 psi for 1 min; 15 min later the sample was again pressed for 1 min. After another 15 min at the same temperature, the sample was slowly cooled to T_g where it was held for 20 min followed by slow cooling to room temperature. While the above procedure is not necessarily optimal, it yielded reasonably consistent results in terms of background fluorescence and fluorescence anisotropies.

For miscible blends this procedure produced optically clear samples with no significant birefringence along the direction in which the pressure was applied. All copolymer/PMMA blends were prepared with this technique as were the copolymer/PEMA blends used to determine $\langle R_g^2\rangle^{1/2}$.

Several copolymer/PEMA samples were prepared by solvent casting from THF. An approximately 30% polymer solution was prepared and placed in the bottom of a glass vial. After drying under nitrogen and then under a vacuum, the glass vials were removed. After three additional days of drying under vacuum, fluorescence depolarization measurements were performed on the samples. Additional drying under vacuum produced no significant change in the time-dependent fluorescence anisotropy. Elemental analysis of samples 600 μm thick after 3 months of drying under vacuum indicated about 15% residual THF.

Data Acquisition. Figure 1 shows the experimental apparatus. The frequency-doubled output of a mode-locked, Q-switched, CW pumped Nd:YAG laser was used to synchronously pump a dye laser. The dye laser was cavity dumped to produce a single pulse at 640 nm which was subsequently doubled to produce a 25-ps, 320-nm excitation pulse. This UV pulse was split with a small fraction being monitored so that the fluorescence intensity could be normalized to the laser intensity. This eliminated the effects of laser intensity drift. Fluorescence from the sample was focused into a monochromator with a polarizer on the entrance slit. A microchannel plate (Hamamatsu R1645U-01) coupled to a transient wave form recorder (Tektronix R7912) detected the polarized fluorescence at 337 nm. A computer was used to store the fluorescence decay and average many decays to improve signal to noise. The time resolution of the detection system was 1 ns.

$I_\parallel(t)$ and $I_\perp(t)$ were obtained by varying the excitation polarization with a half-wave plate. This method of collecting data allows the absolute ratio of $I_\parallel(t)$ to $I_\perp(t)$ to be preserved. For a typical sampale and a given polarization, 2000 fluorescence decays would be averaged by the computer. The polarization of the exciting light would be rotated and another 2000 decays were recorded. After this sequence was repeated, the two decays measured for a particular polarization were compared. The data were kept only if the absolute magnitudes of these two decays were less than 2% different. This procedure assured that an absolute comparison between the parallel and perpendicular data could be made.

Birefringence of the samples would distort the fluorescence anisotropy measurements. We checked for this possibility by placing a polarizer in the excitation beam after the sample and measuring the ratio of the intensities polarized parallel and perpendicular to the original polarization. This ratio was typically 150/1 and never worse than 70/1 except in the phase-separated copolymer/PEMA blends. These ratios are large enough to ensure that the fluorescence anisotropy is not significantly affected.

All the samples had an OD $\leq$ 0.2 at 320 nm. We verified that no significant reabsorption takes place in this range. Typical pulse

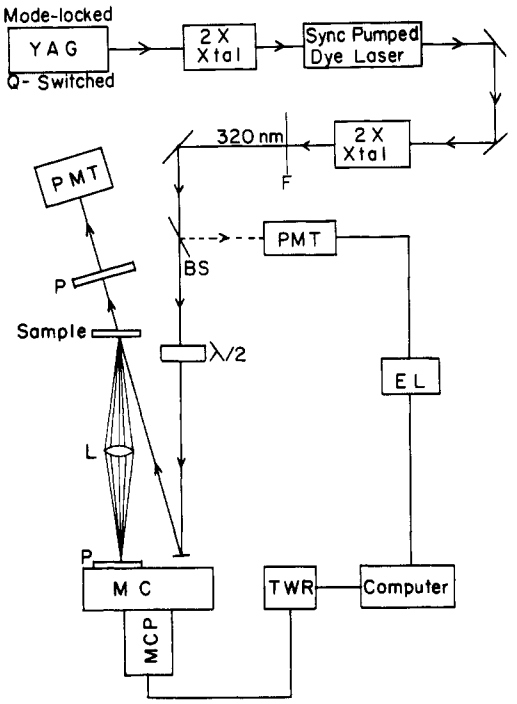

Figure 1. Experimental setup. The doubled output of a mode-locked and Q-switched Nd:YAG laser is frequency doubled and synchronously pumps a dye laser. The dye laser output is doubled to 320 nm for excitation. The polarization of the excitation beam is controlled by a half-wave plate. The fluorescence from the sample is collected by a lens, passed through a polarizer and a monochromator, and detected by a multichannel plate coupled to a transient wave form recorder. See text for further details. BS = beam splitter, PMT = photomultiplier tube, $\lambda/2$ = half-wave plate, EL = electrometer, P = polarizer, L = lens, MC = monochromator, MCP = multichannel plate detector, TWR = transient wave form recorder, F = UV transmitting filter, and 2 × Xtal = second harmonic generating crystal.

energies were ≤ 1 μJ. The dependence of the recorded fluorescence intensity on the excitation intensity was linear, assuring that the microchannel plate was not saturated and that the sample was not being bleached. We checked that our data collection system was not biased with respect to polarization by recording the fluorescence decays of molecules rotating rapidly in solution (2-ethylnaphthalene in THF). The rapid rotation assures that the fluorescence is totally unpolarized. The fluorescence was recorded for both parallel and perpendicular polarization. Since the fluorescence is unpolarized, there should be no fluorescence anisotropy if the detection system is unbiased. The calculation of the fluorescence anisotropy from the data yielded $r(t) = 0.000 \pm 0.005$.

For all except the very lowest copolymer concentrations, fluorescence from the host polymer was negligible compared to the fluorescence from the guest polymer. At very low concentrations we subtracted the digitized background fluorescence from the sample fluorescence to obtain the true fluorescence decays. All measurements were performed at room temperature.

Data Analysis. The experimental $r(t)$ and $G^s(t)$ were obtained from $I_\parallel(t)$ and $I_\perp(t)$ by the point-by-point calculation described in eq 4–6. To accurately compare the experimental $G^s(t)$ with the theoretical predictions, the system's impulse response function must be appropriately convolved with the theoretical $G^s(t)$. This is done by convolving theoretical expressions for $I_\parallel(t)$ and $I_\perp(t)$ (eq 2–4 with $\Phi(t) = 1$) with the system's response function. The theoretical $G^s(t)$ with the convolution is then calculated with eq 5 and 6.

R_0 Determination. For each of the theoretical treatments discussed in section II, $\langle R_g^2\rangle^{1/2}$ is a linear function of R_0. We used the experimental setup described in this section to obtain R_0 in a manner analogous to that used by Gochanour and Fayer.[15] For convenience we used 2-ethylnaphthalene in bulk polymerized PMMA as a model for the naphthalene chromophores on the copolymer chain dispersed in PMMA. We measured the polarized

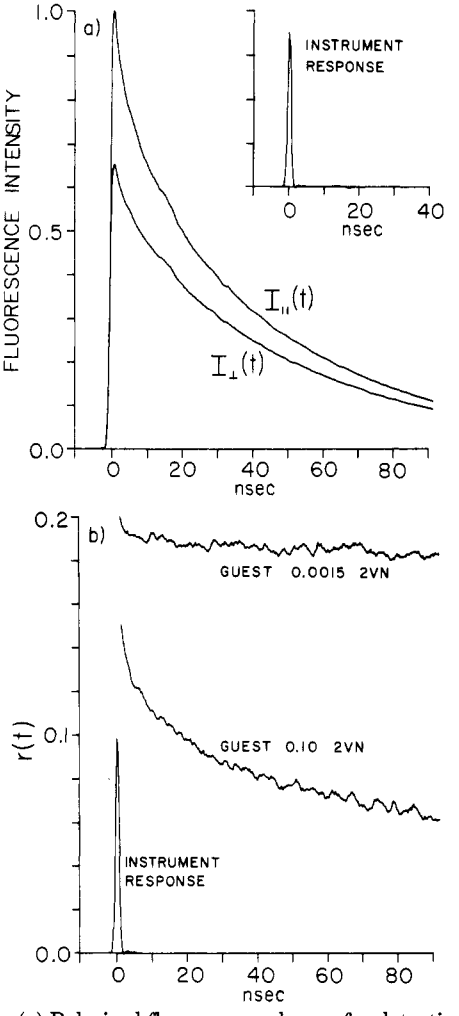

Figure 2. (a) Polarized fluorescence decays for detection parallel ($I_\parallel(t)$) and perpendicular ($I_\perp(t)$) to the excitation polarization. The sample is 20 000 molecular weight copolymer (0.10 mole fraction 2-vinylnaphthalene, 0.90 mole fraction methyl methacrylate) in a 12 000 molecular weight PMMA host. Copolymer concentration is 0.38 wt %. The inset shows the instrumental response of the experimental system. (b) Fluorescence anisotropies, $r(t)$, calculated from $I_\parallel(t)$ and $I_\perp(t)$ (see eq 5). The upper curve is for a copolymer with a very small mole fraction (0.0015) of 2-vinylnaphthalene. Excitation transport does not occur and the time dependence is due to very slow rotational depolarization. The lower curve is for the data displayed in Figure 2a. The time-dependent depolarization is due to excitation transport and the small amount of rotational depolarization (see eq 4). The sharp spike is the instrumental response function.

fluorescence decays for several concentrations of 2-ethylnaphthalene, analyzing the data with eq 4–6. By comparing the data with the theory of Gochanour, Andersen, and Fayer,[12] we determined $R_0 = 13.0 \pm 0.6$ Å. This theory has been shown to be accurate and to directly yield values for R_0 from a transport measurement which are consistent with those determined by spectral overlap measurements.[15,16]

IV. Results and Discussion

PMMA Blends. In order to demonstrate the utility of excitation transport measurements in determining the $\langle R_g^2\rangle^{1/2}$ of a copolymer, our first experiments were performed under approximately Θ-conditions. For such conditions $\langle R_g^2\rangle^{1/2}$ for a homopolymer of the same molecular weight as the copolymer can be easily calculated from tabulated data. The presence of a small fraction of naphthalene chromophores on the chain should not significantly perturb $\langle R_g^2\rangle^{1/2}$.

In Figure 2a we show the polarized fluorescence decays for copolymer I (20 000 molecular weight copolymer, 0.10

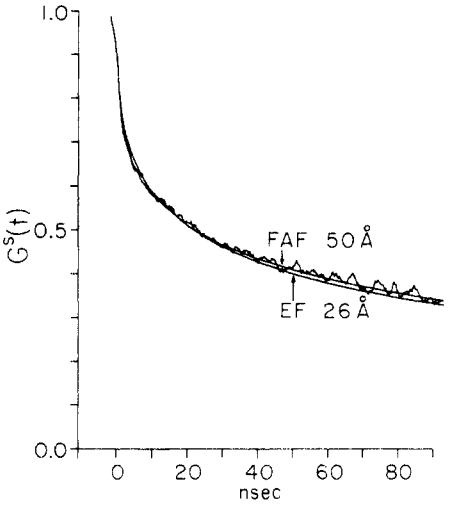

Figure 3. The quantity of theoretical and experimental interest is $G^s(t)$, the ensemble-averaged probability that the excitation is on the originally excited chromophore at time t. The experimental $G^s(t)$ results from taking the ratio of the two anisotropy curves in Figure 2b. The two theoretical curves drawn through the data (EF and FAF) are the best fits for the two theories discussed in the text. The single fitting parameter for each theory gives the $\langle R_g^2\rangle^{1/2}$ as indicated.

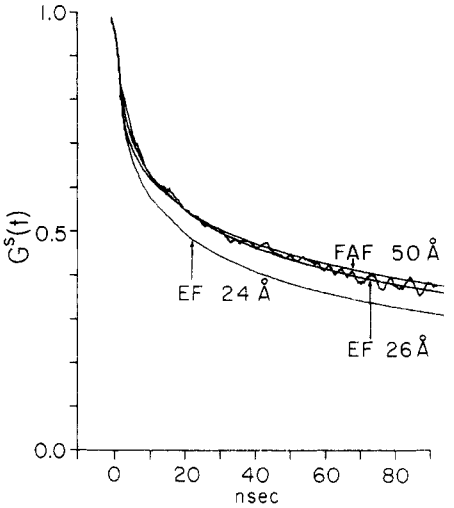

Figure 4. $G^s(t)$, the ensemble-averaged probability of finding the excitation on the originally excited chromophore. The data shown are for the same copolymer as in Figure 3, but the host is 120 000 molecular weight PMMA instead of 12 000 molecular weight PMMA. The bottom curve was calculated for a $\langle R_g^2\rangle^{1/2}$ which is 10% smaller than the best fit to the data. The difference between this curve and the data indicates the sensitivity of this technique to changes in $\langle R_g^2\rangle^{1/2}$. The theoretical curves through the data are for the same parameters as in Figure 3. Within experimental error the copolymer does not change size when the molecular weight of the host is increased by 1 order of magnitude.

mole fraction 2-vinylnaphthalene, 0.90 mole fraction methyl methacrylate) in a 12 000 molecular weight PMMA host. The copolymer concentration is 0.38 wt %. By performing fluorescence polarization measurements on samples of various guest concentrations, we determined that a negligible amount of transport between chromophores on different chains occurs at this concentration. The absence of any significant eximer emission indicates that there is no aggregation of naphthalene chromophores at these low concentrations. In Figure 2b the lower curve is the fluorescence anisotropy calculated from $I_{\parallel}(t)$ and $I_{\perp}(t)$ (see eq 5) shown in Figure 2a. The upper curve is $r(t)$ for copolymer II (0.0015 mole fraction 2-vinylnaphthalene) in the same host material. Copolymer II contains so few chromophores that only depolarization due to motion of the chromophore is observed. In this case $r(t)$ is almost flat as expected for a PMMA matrix far below T_g. As discussed in section II, $G^s(t)$ for copolymer I is given by the ratio of the lower and upper curves in Figure 2b. The experimental $G^s(t)$ obtained in this way is shown in Figure 3. In Figure 4 we show $G^s(t)$ for the same copolymer dispersed in a 120 000 molecular weight PMMA host. The two experimental $G^s(t)$ curves are not significantly different compared to experimental errors arising from a slight lack of reproducibility in the sample preparation.

Figures 3 and 4 also show the best single parameter fits for the EF and FAF theories convolved with the detection system's response function. Both theoretical treatments correctly describe the time dependence of the experimental data. However, the values for $\langle R_g^2\rangle^{1/2}$ for the two theories are very different. The EF theory yields 26 Å while the FAF theory yields 50 Å. For comparison a wide variety of experimental techniques yield a value of 37 ± 4 Å for a 20 000 molecular weight PMMA homopolymer.[17]

The explanation for the disparity between the values for $\langle R_g^2\rangle^{1/2}$ obtained from the theoretical curves and the expected value is straightforward. Neither theory incorporates the proper chromophore pair correlation function for a 20 000 molecular weight chain of PMMA. In Figure 5 we show reduced radial pair correlation functions for the two theoretical approaches. The FAF line is the limiting value for an infinite chain and is given by eq 3.2 of ref 3.

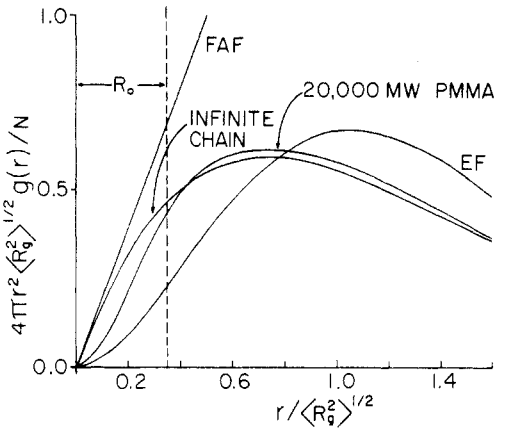

Figure 5. Reduced radial pair correlation functions. The curves labeled FAF and EF are for the pair correlation functions contained in the FAF and EF theories used to fit the data in Figures 3 and 4. The other two curves were obtained by performing a sum over statistical segments, assuming Gaussian bond probabilities. The curve labeled "Infinite Chain" is the result of this sum in the limit of a large number of segments. The curve for a 20 000 molecular weight PMMA chain was obtained by summing over 32 statistical segments of length 16 Å. Neither FAF nor EF correctly describes the pair correlation function in the region of interest ($\lesssim 0.35\langle R_g^2\rangle^{1/2}$). Larger radial values do not contribute appreciably to excitation transport as they correspond to distances $> R_0$, the critical transfer radius for excitation transport. The line indicating R_0 (13 Å for naphthalene) is located for an $\langle R_g^2\rangle^{1/2}$ of 37 Å, appropriate for 20 000 molecular weight PMMA.

The EF correlation function is not the basis for the excitation transfer calculation in their theory, but is implicit in their model. (The calculation of this correlation function is discussed in Appendix B.)

Two other correlation functions are shown in Figure 5. Both were calculated by performing a double sum over the statistical segments of an ideal PMMA chain assuming Gaussian bond probabilities. The curve designated as the infinite-chain result was obtained by this procedure in the limit of a very large number of statistical segments. The curve labeled "20 000 MW PMMA" was obtained by sum-

ming over 32 statistical segments (see Appendix B for details). Note that at distances less than $0.1\langle R_g^2\rangle^{1/2}$ the FAF correlation function is a very good approximation to the result for sufficiently large chains.

Excitation transport is unlikely between two chromophores separated by a distance significantly greater than R_0. Hence, only a part of the pair correlation function is required to calculate fluorescence depolarization observables. (As a result, excitation transport measurements do not provide direct information about the pair correlation function for distances significantly larger than R_0.)

R_0 for the naphthalene chromophore on this copolymer is indicated in the figure. At distances $\leq R_0$, neither the FAF nor EF theory correctly describes the pair correlation function for a 20 000 molecular weight chain of PMMA. The EF theory underestimates the concentration of nearby chromophores. The best theoretical fit to the data compensates for this by making $\langle R_g^2\rangle^{1/2}$ too small, thus increasing the local chromophore concentration. The FAF theory overestimates the local chromophore concentration for this finite chain, and hence overestimates $\langle R_g^2\rangle^{1/2}$. The true pair correlation function for the 20 000 molecular weight polymer lies roughly halfway between the FAF and EF curves. This is consistent with the fact that the expected $\langle R_g^2\rangle^{1/2}$ (37 ± 4 Å) is halfway between the values obtained from the data by the theories.

We can obtain a quantitative estimate of $\langle R_g^2\rangle^{1/2}$ from the data in Figures 3 and 4 by the following procedure. We can match the FAF curve to the correct pair correlation function (at distances $\leq R_0$) by multiplying the FAF correlation function by about 0.5. This is equivalent to replacing N by $0.5N$ in eq A8 in Appendix A. This makes $\langle R_g^2\rangle^{1/2}$ smaller by a factor of $1/2^{1/2}$, yielding a value of 35 Å in very good agreement with the expected result. (A similar argument can be made for the EF curve also yielding a value for $\langle R_g^2\rangle^{1/2}$ of 35 Å.)

The above arguments clearly demonstrate that the discrepancy between the values for $\langle R_g^2\rangle^{1/2}$ calculated by the theoretical fits to the data and the accepted value is due to the inapplicability of the two theories to a polymer of this molecular weight. On the basis of this argument, we believe that a theory which employs the proper correlation function would yield an accurate value of $\langle R_g^2\rangle^{1/2}$. Further theoretical work is in progress. Additional experiments will be performed on a copolymer of the same molecular weight but with fewer chromophores. These experiments will determine whether the presence of a small fraction of chromophores in the PMMA backbone significantly perturbs the chain structure. Such experiments will also ensure that the chromophore concentration is low enough to eliminate any bias toward transport along the chain.[1,2]

Two more points should be made about the comparison of the data in Figures 3 and 4 with the theoretical curves. First, excitation transport is a very sensitive measure of $\langle R_g^2\rangle^{1/2}$. The bottom curve in Figure 4 was calculated for a $\langle R_g^2\rangle^{1/2}$ which is 10% smaller than the best fit to the data. The large difference between this curve and the data indicates the sensitivity of this technique to changes in $\langle R_g^2\rangle^{1/2}$.

Second, the fact that the theoretical approaches correctly describe the time dependence of the excitation transport data in Figures 3 and 4 is significant. In Figure 6 we show the same experimental data as in Figure 4. The smooth curves are the theoretical results of Gochanour, Andersen, and Fayer[12] for excitation transport among chromophores randomly distributed in solution. The various curves correspond to different concentrations. These theoretical

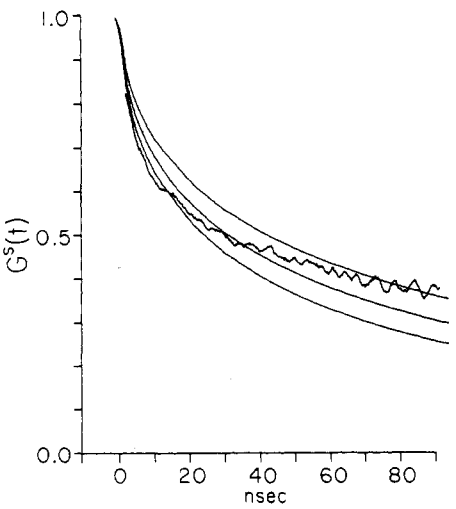

Figure 6. Experimental data of Figure 4 and theoretical curves calculated by using an accurate theory for excitation transport among chromophores randomly distributed in solution. The curves are for various concentrations. The solution theory cannot reproduce the functional form of the time-dependent excitation transport for any choice of the concentration.

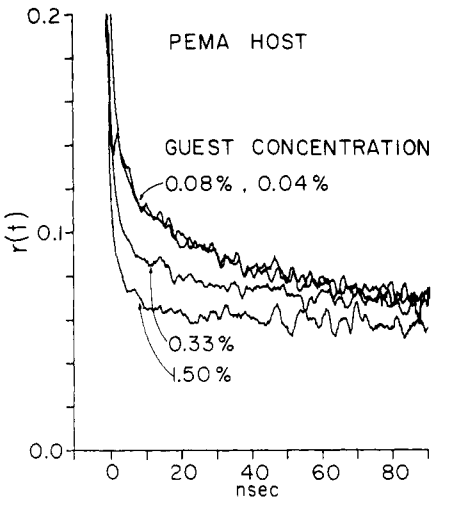

Figure 7. Concentration dependence of the fluorescence anisotropy of a methyl methacrylate/2-vinylnaphthalene copolymer in a PEMA host. $G^s(t)$ (and hence $r(t)$) is sensitive to coil aggregation because of changes in the local chromophore concentration. The 1.5% sample was visibly clouded, indicating phase separation; $r(t)$ decays quite rapidly because of high local chromophore concentration. As the concentration is decreased, $r(t)$ decays more slowly because of lower local chromophore concentrations. When $r(t)$ becomes independent of concentration (0.08% for this system), the coils are isolated and the blend is miscible. For an isolated coil excitation transport only occurs among chromophores on the coil. Hence, $r(t)$ is independent of the copolymer concentration in the blend.

results have been shown to accurately describe excitation transport in a solution of randomly distributed chromophores.[15] No value of the concentration yields a curve which matches the shape of the experimental data. The fact that both the EF and FAF theories correctly describe the shape of the data indicates that the essential features of the polymer statistics have been incorporated into these theoretical approaches.

PEMA Blends. We also performed fluorescence depolarization measurements on blends of the methyl methacrylate/2-vinylnaphthalene copolymers with poly(ethyl methacrylate) (PEMA). When prepared by solvent casting from THF, these blends were phase separated except at very low copolymer concentrations.

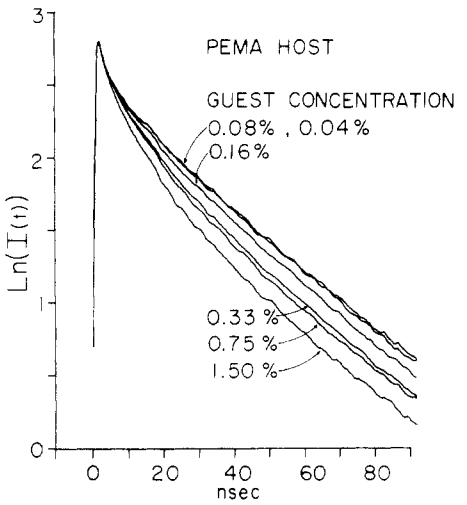

Figure 8. Concentration dependence of the excited-state lifetime decay of a methyl methacrylate/2-vinylnaphthalene copolymer in a PEMA host. The decreased lifetime at high guest concentrations is probably due to trapping by interchain alkylnaphthalene dimers. As in Figure 7, these results demonstrate that the blend becomes miscible at concentrations below 0.08%.

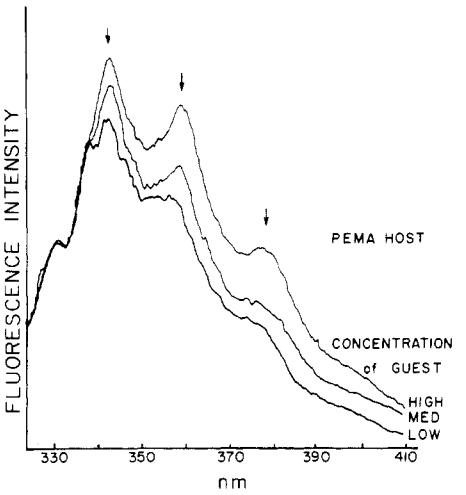

Figure 9. Concentration dependence of the emission spectra of a methyl methacrylate/2-vinylnaphthalene copolymer in a PEMA host. At high guest concentrations (phase separation), interchain alkylnaphthalene dimers trap and subsequently emit. The three new bands in the emission spectra at high guest concentrations match the three bands reported by Irie et al. (see arrows) in the emission spectra of poly(2-vinylnaphthalene) which are attributed to dimer emission.

In Figure 7 we show the fluorescence anisotropy of several copolymer/PEMA blends as a function of the copolymer concentration. The guest is the 20 000 molecular weight copolymer (0.90 methyl methacrylate and 0.10 2-vinylnaphthalene) in 120 000 molecular weight PEMA host. The blend with the highest copolymer concentration (1.5%) was visibly clouded, indicating phase-separated domains of at least tenths of microns. The fluorescence anisotropy for this concentration decays much faster than for lower copolymer concentrations. This indicates relatively fast excitation transport, since $G^s(t)$ is roughly proportional to $r(t)$ when there is little chromophore motion (see eq 4). The fast transport is due to the high local chromophore concentration in the phase-separated domains. As the concentration of the copolymer in the blend is lowered, excitation transport becomes less likely, presumably because a larger and larger fraction of the copolymer is present in a PEMA-rich phase. (The anisotropy curves at intermediate concentrations contain information about the structure of phase-separated domains. The quantitative interpretation of such curves requires a theoretical treatment which models the nature of the phase-separated domains.) At copolymer concentrations $\leq 0.08\%$ the rate of excitation transport is independent of concentration. Thus, at these concentrations the copolymer coils are isolated and the blend is miscible.

This interpretation of the concentration dependence of $r(t)$ is consistent with two other sets of experimental observations. In these solvent cast blends some form of trapping of the electronic excitation takes place. Hence, there is a concentration dependence in the lifetime decay of the naphthalene chromophores as well as in the steady-state emission spectra. Figure 8 shows the lifetime decays as a function of the copolymer concentration. The decays were obtained with the angle between the excitation and emission polarizations set to the magic angle.[18] This eliminates time-dependent depolarization effects from the fluorescence decay data. At the higher concentrations the decay is strongly nonexponential and much faster than at lower concentrations. The fast decays are due to trapping which occurs at the high local chromophore concentrations associated with phase separation. As the copolymer concentration is decreased, trapping becomes less efficient until the concentration is $\leq 0.08\%$, where no further changes are detected. Note that the concentration at which the experiments indicate the blends become miscible is identical for the two types of measurements illustrated in Figures 7 and 8.

In Figure 9 we show the emission spectra of blends of various copolymer concentrations. As the copolymer concentration is increased and the coils begin to aggregate, three new bands grow into the emission spectra. These bands are characteristic of trap emission. They provide important evidence as to the identity of the trapping species. Figure 9 also shows three arrows at wavelengths where Irie et al.[19] have reported emission bands from poly(2-vinylnaphthalene) in solution. They were able to show that these emission bands are due to a ground-state dimer formed by two of the naphthalene units on the chain. The correspondence between the arrows and the new emission bands shown in our data is strong evidence that ground-state dimers are responsible for the excitation trapping in phase-separated domains. (It is also possible that the traps are unsaturated vinylnaphthalene end groups.)

The precise identity of the trapping species is not important for the interpretation of the data presented in this section. The concentration dependence of the trapping indicated in Figure 8 is completely consistent with the excitation transport shown in Figure 7. Both experiments indicate that the solvent cast PEMA blends are miscible at methyl methacrylate/2-vinylnaphthalene copolymer concentrations $\leq 0.08\%$.

The determination of $\langle R_g^2 \rangle^{1/2}$ for the copolymer in PEMA was more difficult than for the PMMA blends. In order to ensure that the depolarization due to chromophore motion was appropriately handled, it was necessary to put the copolymer with a very small fraction of chromophores into a PEMA host. The copolymer concentration had be $<0.08\%$ to assure that phase separation would not occur. At such low chromophore concentrations background fluorescence from the host PEMA (molecular weight $\simeq$ 12 000) was not negligible. By carefully subtracting the background fluorescence for each polarization, we were able to estimate the depolarization due to chromophore motion in the PEMA blends.

We also determined the fluorescence anisotropy for the copolymer with 0.10 mole fraction 2-vinylnaphthalene in

the 12 000 molecular weight PEMA at copolymer concentration ≤0.08%. From comparing the experimental $G^s(t)$ with calculated curves from the EF theory, we determined $\langle R_g^2\rangle^{1/2} = 28 \pm 3$ Å. The value for the identical copolymer in the PMMA host is 26 ± 2 Å. Thus, $\langle R_g^2\rangle^{1/2}$ for the copolymer in the two different hosts is not significantly different within the experimental errors.

As discussed above, the $\langle R_g^2\rangle^{1/2}$ obtained is somewhat low because of the nature of the pair correlation function implicit in the EF theory. However, the comparison of the copolymer sizes in the two blends is valid as the error in the pair correlation function should be essentially the same in the analysis of the two materials. In future experiments the size of the errors in the measurements should be greatly reduced as they arise mainly from problems with sample preparation rather than from any inherent limitation of the technique.

V. Concluding Remarks

In this paper we have applied electronic excitation transport experiments to the study of polymer blends. It was shown that when the chromophore-containing polymer (guest) is in low concentration, the excitation transport experiments provide a sensitive probe of the size of isolated guest coils. Recent theoretical treatments are able to accurately describe the time dependence of fluorescence depolarization produced by excitation transport. If an appropriate pair correlation function is combined with the existing theoretical approaches, quantitative determination of coil size should be possible. This approach may prove invaluable in situations in which light-scattering and neutron-scattering methods are not applicable, particularly in low-concentration blends.

At higher guest concentrations phase separation was manifested as increased rates of fluorescence depolarization and decreased excited-state lifetimes. Both occur because of higher local chromophore concentration in the phase-separated regions which have high guest concentration. The higher chromophore concentration in the guest-rich domains results in faster excitation transport, and in trapping by dimers of the chromophores. The increased rate of transport and the appearance of concentration-dependent trapping indicate that the guest coils are intertwined in the guest-rich domains.

In addition to providing information on coil size and aggregation in blends, time-resolved fluorescence depolarization measurements should be useful in studying a variety of other polymer problems. Changes in coil size in different hosts and with solvent fraction in concentrated solutions can be investigated. The effects of sample preparation on coil structure can be examined. Changes in coil size upon annealing blends of unusual conformations after freeze-drying will be manifested in the excitation dynamics.

The fluorescence depolarization observables are critically dependent on the local environments of the coil chromophores. Since excitation transport is very sensitive to even small changes in the spatial distribution of chromophores and because fluorescence experiments are capable of detecting very small concentrations of chromophores, the experimental and theoretical methods discussed in this paper represent a new approach to the investigation of polymer blend structure.

Acknowledgment. We thank Dr. Glenn Fredrickson and Prof. Curtis Frank for many valuable discussions, and we thank Prof. Frank for providing the 10% 2-vinylnaphthalene/methyl methacrylate copolymer. This work was supported by the Department of Energy, Office of Basic Energy Sciences (DE-FG03-84ER13251). Additional equipment support was provided by the National Science Foundation, Division of Materials Research (DMR 84-16343) and the Stanford National Science Foundation Center for Materials Research.

Appendix A

In this appendix we provide the equations needed to calculate the theoretical expressions for $G^s(t)$. Both the EF and FAF theories develop expressions for the Laplace transform of $G^s(t)$. The inverse Laplace transform was performed numerically by using the Stehfest algorithm.[20]

In the EF theory[1]

$$\langle \hat{G}^s(N,\langle R_g^2\rangle^{1/2},\epsilon)\rangle = \int_0^\infty dR_g\, P(R_g)\hat{G}^s(N,\beta,\epsilon) \quad \text{(A1)}$$

where N is the number of chromophores on the chain and ϵ is the Laplace variable. The Flory–Fisk distribution function $P(R_g)$ is given by

$$P(R_g) = \left(\frac{343}{15}\right)\left(\frac{14}{\pi\langle R_g^2\rangle}\right)^{1/2}\left(\frac{R_g^2}{\langle R_g^2\rangle}\right)^3 \exp\left(-\frac{7R_g^2}{2\langle R_g^2\rangle}\right) \quad \text{(A2)}$$

The other relations needed to evaluate eq A1 are

$$\hat{G}^s(N,\beta,\epsilon) = \epsilon^{-1}\left\{1 + \frac{C_D}{(\epsilon\tau)^{1/2}}\left(1-\frac{1}{N}\right)f_2(\beta) + \frac{C_D^2}{\epsilon\tau}\left(1-\frac{1}{N}\right)\left[\left(1-\frac{1}{N}\right)(f_2(\beta))^2 - \left(1-\frac{2}{N}\right)f_3(\beta)\right]\right\}^{-1} \quad \text{(A3)}$$

$$\beta = (5/3)^{3/2}(R_g/R_0)^3(\epsilon\tau/2)^{1/2} \quad \text{(A4)}$$

$$C_D = (3/5)^{3/2}N(R_0/R_g)^3 \quad \text{(A5)}$$

$f_2(\beta)$ and $f_3(\beta)$ are analytical functions presented in the appendix of ref 21. In order to account for the orientation dependence of the transfer rate, R_0 in the above equations must be replaced by $(\gamma_3)^{1/3}R_0$, where $\gamma_3 = 0.8452$.[3,13,21]

We used the three-body rational approximation[5] to calculate the Laplace transform of $G^s(t)$ from the FAF theory. By eliminating all terms due to excitation trapping and terms due to transfer among chromophores on different chains, we obtained the following result:

$$\epsilon\hat{G}^s(\epsilon,\bar{C}_D) = \frac{1 - 0.7721\bar{C}_D[\hat{G}^s(\epsilon,\bar{C}_D)/\tau]^{1/3}}{1 + 0.6827\bar{C}_D[\hat{G}^s(\epsilon,\bar{C}_D)/\tau]^{1/3}} \quad \text{(A6)}$$

where the explicit dependence of $\hat{G}^s$ on the reduced concentration $\bar{C}_D$ has been indicated. $\bar{C}_D$ is defined by

$$\bar{C}_D = \pi q_D(R_0/a)^2 \quad \text{(A7)}$$

where a is the length of a statistical segment and q_D is the average number of chromophores on a statistical segment. Note that eq A6 must be iterated with respect to ϵ.

For an ideal chain it is possible to relate $\bar{C}_D$ to $\langle R_g^2\rangle^{1/2}$ by[6]

$$\langle R_g^2\rangle^{1/2} = R_0(N\pi/6\bar{C}_D)^{1/2} \quad \text{(A8)}$$

where N is the number of chromophores on the chain. In the FAF theory the orientation dependence of the transfer rate is incorporated by replacing R_0 by $(\gamma_2)^{1/2}R_0$ in eq A7 and A8 ($\gamma_2 = 0.8468$).[3]

Appendix B

In this appendix we calculate three of the correlation functions in Figure 5. The two calculations involving

statistical segments use the following form for the chromophore pair correlation function of an ideal chain:[3]

$$g(\vec{r}) = \frac{N}{\bar{N}(\bar{N}-1)} \sum_{\substack{i=1 \\ i \neq j}}^{\bar{N}} \sum_{j=1}^{\bar{N}} P_{ij}(\vec{r}) \qquad \text{(B1)}$$

In this expression N is the number of chromophores on the chain, $\bar{N}$ is the number of statistical segments in the chain, and the bond probabilities are taken to be Gaussian[2,22]

$$P_{ij}(\vec{r}) = \left(\frac{3}{2\pi a^2|i-j|}\right)^{3/2} \exp\left(\frac{-3r^2}{2a^2|i-j|}\right) \qquad \text{(B2)}$$

The statistical segment length is denoted by a.

Based on a value of C_∞ of 8.65 for PMMA,[17] the statistical segment length was calculated to be 16 Å with 6.3 monomers per statistical segment. To calculate the chromophore pair correlation function for a 20 000 molecular weight PMMA chain, the sum in eq B1 was performed numerically with $\bar{N} = 32$. To calculate the pair correlation function for an infinite chain, we performed the sum in eq B1 with successively larger values of N until the result converged.

The correlation function implicit in the EF theory was calculated by first obtaining the pair correlation function for N chromophores randomly distributed in a sphere with a second moment of R_g. (See eq 9 of ref 1.) This result, designated $g(\vec{r},R_g)$, is

$$g(\vec{r},R_g) = \frac{3N}{64\pi(5/3)^{3/2}R_g^3}\left[16 - \frac{12r}{(5/3)^{1/2}R_g} + \frac{r^3}{(5/3)^{3/2}R_g}\right]\Theta(2(5/3)^{1/2}R_g - r) \qquad \text{(B3)}$$

where $\Theta(x) = 1$ for $x > 0$ and zero for $x < 0$.

To obtain the final result we average over the distribution function of R_g

$$g(\vec{r}) = \int_0^\infty dR_g\, P(R_g) g(\vec{r},R_g) \qquad \text{(B4)}$$

where $P(R_g)$ is given by eq A2.

Registry No. PMMA (homopolymer), 9011-14-7; PEMA (homopolymer), 9003-42-3; (vinylnaphthalene)·(methyl methacrylate) (copolymer), 53640-71-4.

References and Notes

(1) M. D. Ediger and M. D. Fayer, *Macromolecules*, **16**, 1893 (1983).
(2) G. H. Fredrickson, H. C. Andersen, and C. W. Frank, *Macromolecules*, **16**, 1456 (1983).
(3) G. H. Fredrickson, H. C. Andersen, and C. W. Frank, *Macromolecules*, **17**, 54 (1984).
(4) G. H. Fredrickson, H. C. Andersen, and C. W. Frank, *J. Chem. Phys.*, **79**, 3572 (1983).
(5) G. H. Fredrickson, H. C. Andersen, and C. W. Frank, *Macromolecules*, **17**, 1496 (1984).
(6) G. H. Fredrickson, H. C. Andersen, and C. W. Frank, *J. Polym. Sci., Polym. Phys. Ed.*, **23**, 591 (1985).
(7) R. Ullman, *Ann. Rev. Mater. Sci.*, **10**, 261 (1980).
(8) C. W. Frank and M. A. Gashgari, *Ann. N.Y. Acad. Sci.*, **366**, 387 (1981).
(9) C. W. Frank, M. A. Gashgari, P. Chutikamontham, and V. J. Haverly, *Stud. Phys. Theor. Chem.*, **10**, 187 (1980).
(10) J. Jachowicz and H. Morawetz, *Macromolecules*, **15**, 828 (1982).
(11) Th. Förster, *Ann. Phys.*, **2**, 55 (1948).
(12) C. R. Gochanour, H. C. Andersen, and M. D. Fayer, *J. Chem. Phys.*, **70**, 4254 (1979).
(13) M. D. Ediger, R. P. Domingue, and M. D. Fayer, *J. Chem. Phys.*, **80**, 1246 (1984).
(14) T. G. Fox, J. B. Kinsinger, H. F. Mason, and E. M. Schuele, *Polymer*, **3**, 71 (1962).
(15) C. R. Gochanour and M. D. Fayer, *J. Phys. Chem.*, **85**, 1989 (1981).
(16) R. J. D. Miller, M. Pierre, and M. D. Fayer, *J. Chem. Phys.*, **78**, 5183 (1983).
(17) M. Jurata, Y. Tsunashima, M. Iuama, and K. Kamada in "Polymer Handbook", J. Brandrup and E. H. Immergut, Eds. Wiley-Interscience, New York, 1975, p IV-38.
(18) E. D. Cehelnik, K. D. Mielenz, and R. A. Velapoldi, *J. Res. Natl. Bur. Stand., Sect. A*, **79**, 1 (1975).
(19) M. Irie, T. Kamijo, M. Alkaua, T. Takemura, K. Hayashi, and H. Baba, *J. Phys. Chem.*, **81**, 1571 (1977).
(20) H. Stehfest, *Commun. Assoc. Comput. Mach.*, **13**, 47, 624 (1970).
(21) M. D. Ediger and M. D. Fayer, *J. Chem. Phys.*, **78**, 2518 (1983).
(22) H. Yamakawa, "Modern Theory of Polymer Solutions", Harper and Row, New York, 1971.
(23) P. J. Flory, "Statistical Mechanics of Chain Molecules", Wiley, New York, 1969, p 12.